# RELATIVE PERFORMANCE COMPARISON BETWEEN BASELINE LABYRINTH AND DUAL-BRUSH COMPRESSOR DISCHARGE SEALS IN A T-700 ENGINE TEST



Robert C. Hendricks
NASA Lewis Research Center
Cleveland, Ohio

Thomas A. Griffin
Vehicle Propulsion Directorate
U.S. Army Research Laboratory
NASA Lewis Research Center
Cleveland, Ohio

Kristine R. Csavina
Sverdrup Technology, Inc.
NASA Lewis Research Center Group
Brook Park, Ohio

and

Arvind Pancholi and Dvandra Sood
General Electric Corporation
Lynn, Massachusetts

## ABSTRACT

In separate series of T–700 engine tests, direct comparisons were made between the forward-facing labyrinth and dual-brush compressor discharge seals. Compressor speeds to 43 000 rpm, surface speeds to 160 m/s (530 ft/s), pressures to 1 MPa (145 psi), and temperatures to 680 K (765 °F) characterized these tests. The wear estimate for 40 hr of engine operations was less than 0.025 mm (0.001 in.) of the Haynes 25 alloy bristles running against a chromium-oxide-coated rub runner. The pressure drops were higher for the dual-brush than for the forward-facing labyrinth seal, implying better seal characteristics and engine performance for the brush seal. Modification of the secondary flow path requires that changes in cooling air and engine dynamics be accounted for.

## INTRODUCTION

Labyrinth seals are efficient, readily integrated into designs, and generally easy to install into engines but are inherently unstable (Hendricks et al., 1992). However, installing a simple swirl break significantly enhances the stability margin and mitigates this drawback (Childs et al., 1989). Details of theory, experiments, and design methods for labyrinth seals and configurations are provided by Trutnovsky (1977). Forward-facing labyrinth tooth configurations with a variety of rub interfaces (e.g., honeycomb) were studied in detail by Stocker et al. (1977) under a U.S. Air Force contract with codes developed by Morrison and Chi (1985), Demko et al. (1988), and Rhode et al. (1988) and by Rocketdyne (internal Rocketdyne report). Optimization procedures are available from MTI Inc. (private communication from W. Shapiro) and are being implemented into the NASA seals codes program.

Brush seal systems are efficient, stable, contact seals that are usually interchangeable with labyrinth shaft seals but require a smooth rub runner interface and an interference fit upon installation. The major unknowns and needed research are tribological (e.g., life or interface friction and wear) because of the following performance demands: pressure drops over 2.1 MPa (300 psi), temperatures to over 1090 K (1500 °F), and surface speeds to 460 m/s (1500 ft/s). Current research supported by the Navy (private communication from W. Voorhees), the U.S. Army (private communication from R. Bill and G. Bobula), and the U.S. Air Force's Wright Patterson Air Force Base is addressing these issues and shows promise in meeting these demands.

In this paper we compare the relative pressure drop differences between the baseline labyrinth and dual-brush compressor discharge seals at compressor discharge pressures to 1 MPa (145 psi) and temperatures to 680 K (765 °F) with operating speeds to 43 000 rpm.

## ENGINE FLOW PATH

The power stream airflow through the compressor and the secondary airflow leakage past the compressor discharge seal are illustrated in Fig. 1. The compressor discharge seal package and associated drain tube are located immediately downstream of the impeller and labeled CDS. The drain tube was opened after a series of runs and swabbed for debris.

## COMPRESSOR DISCHARGE SEAL

### Labyrinth Seal System

The nominal 71-mm (2.8-in.) diameter forward-facing labyrinth seal system is illustrated in Fig. 2. The labyrinth teeth rub into a felt-metal type of interface, forming the seal system. Note that the teeth are not all forward facing and are used in different ways to satisfy different engine operating requirements. A simulated exploded view of the seal system is given in Fig. 3 and clearly illustrates the forward-facing teeth of the rotor. However, the housing shown in the figure is for the brush seal.

### Brush Seal System

The brush seal system replacement package is illustrated in Fig. 4. The dual brush, nominally 71 mm (2.8 in.) in diameter, runs against a chromium-oxide-coated rub runner interface as shown schematically. The basic seal system was envisioned by General Electric and manufactured by Cross Mfg. Ltd. (Flower, 1990). It has 0.071-mm (0.0028-in.) diameter, Haynes 25 bristles angled 43° to 50° to the interface with approximately 98 to 99 per millimeter of circumference (2500 per inch of circumference) and a nominal interference fit of 0.127 mm (0.005 in.) at installation. Figure 5 gives a post-test exploded view of the brush seal system with associated instrumentation lines (cut after testing). Figure 6 provides a side-by-side comparison of the forward-facing labyrinth seal (right) and the chromium-oxide-coated rub runner replacement (left); these represent the rotating interface.

## APPARATUS AND INSTRUMENTATION

Pretest and post-test photographs of the dual brush and its installation in the seal system are shown as a series in Fig. 7. Figure 8 depicts the dual brush prior to testing. Figure 7(a) shows the upstream view of the instrumented housing; four thermocouples are attached to the side plates with upstream and downstream pressure taps. Figure 7(b) shows a direct view from the downstream side, and Fig. 7(c) is an isometric view showing the "shiny" nature of the bristle interface. Actual brush seal dimensions, rub runner coating, and installation of instrumentation are proprietary.

## ENGINE SEAL INSTALLATION AND OPERATIONS

The T–700 compressor section was first assembled with the labyrinth seal and run as a baseline for comparison. After a test series was completed, the engine was shipped to the Corpus Christi overhaul facility. The compressor discharge seal labyrinth system was removed and the brush seal system was installed. The brush seal system was installed without special waxes, which can lead to bristle distortions and irregular bristle voidage. These waxes hold the bristles off the rotor during installation and readily "burn out" at a low temperature.

Operations consisted of the standard break-in procedures with data taken primarily under steady conditions. The engine was operated a total of 20 hr, including break-in, from ground to flight idle. Compressor speeds were to 43 000 rpm with seal housing temperatures to 680 K (765 °F). Local conditions at various compressor discharge pressures are given in Table I. The compressor discharge seal leakage was vented through the drain tube (Fig. 1) and metered by using a calibrated orifice. Because leakage data results were noisy, pressure drop was judged a more reliable indicator of leakage. The debris collected in the drain tube was a "lubricant powder," but the spectra indicated several contaminant metals from elsewhere in the engine. Rotor roughness, brush construction, and upstream debris generation play a major role in determining the spectrum. Although neither radial nor axial rotor positions were monitored, such position sensors should be an integral part of the engine dynamics.

## RESULTS

Post-test measurements of the brush and inspection of the bristles revealed a smooth bristle interface with some characteristic shear wear (Fig. 9) but little other visible damage. The brush wear patterns (Figs. 10 and 11) were attributed to the engine dynamics although no dynamic tracking instrumentation was available. The patterns are interesting in that they are 15° from the antirotation pin. (GE is to provide clocking and determine if that point is associated with a compressor bearing position or loading point.) The patterns for the upstream seal differed from those for the downstream seal (see also Fig. 4), indicating a differential in pressure drop across each of the seals. It is anticipated that about 40 percent of the total pressure drop across the dual brush occurred across the first brush and 60 percent across the second brush (Flower, 1990, and private communication from R. Flower of Cross Mfg. Ltd.). Such loading resulted in stiffer bristles in the second brush and implies a greater bristle wear. Preload and operational loads are important design life parameters (private communication from Wright Patterson Air Force Base), but data to quantize these parameters are not available.

Another variation in the wear pattern is attributed to the rotor machining or coating variations (Fig. 11). The rotor showed a small eccentricity and was investigated for metallic transfer, but no significant transfer was found. The chromium oxide interface was worn smoother by the rubbing brush bristle interface, implying some form of wear or material smearing without significant transfer of the chromium oxide (CrO).

During the test series the drain pipe (Fig. 1) was swabbed for debris. When these samples were in turn investigated with a scanning electron microscope (SEM), nickel, chromium, and tungsten lines were observed along with other unexplainable peaks of salts (e.g., Fig. 12). The nickel, chromium, and tungsten lines characterize bristle materials and some possible coating wear. The debris was fine and difficult to locate and isolate within the tube. Other metal sources and rubbing surfaces could have also produced such debris, but we attributed it to bristle wear.

The CrO-coated rub runner exhibited slight wear scars but no spallation or coating degradation otherwise. These wear bands are readily visible in Fig. 6, where the upper band is associated with the upstream (high-pressure side) brush; see also Fig. 5. The upstream wear surface is characterized by Fig. 13(a) and the downstream wear surface by Fig. 13(b). The CrO coating is characterized by light and gray areas, and the energy spectrum shows the light areas to be an NiCr composition and the gray areas to be predominantly Cr. The light and gray areas of the matrix or unrubbed material between the bands is illustrated in Figs. 13(c) and (d). Similarly, for the upstream wear band in Figs. 13(e) and (f) and for the downstream wear band in Figs. 13(g) and (h). There appears to be no material transfer from the bristles to the rotor and only minor scarring and polishing.

The result of interest here is that the initial design interference was 0.127 mm (0.005 in.) and the post-test estimate of interference was 0.101 mm (0.004 in.), or perhaps a maximum wear of 0.025 mm (0.001 in.).

Although direct flow measurements were not available, the pressure drops for each comparable compressor discharge pressure setting were higher for the brush seal system than for the labyrinth seal system (Tables I and II). The implication is that for the same engine

operating conditions the dual-brush system leaked less than the baseline forward-facing labyrinth seal system. Also implied is enhanced engine efficiency.

It is important to recognize that more efficient seals cannot simply be installed without computing and accounting for the secondary airflows necessary for the cooling and engine dynamics associated with the seal leakage modifications.

## SUMMARY

In a series of T–700 engine tests, direct comparisons were made between a forward-facing labyrinth seal configuration and a dual-brush compressor discharge seal. The nominal seal diameter was 71 mm (2.8 in.). The test conditions included compressor discharge pressures to 1 MPa (145 psi), temperatures to 680 K (765 °F), operating speeds to 43 000 rpm, and surface speeds to 160 m/s (530 ft/s) with the working fluid being nominally dry ambient air. The bristle wear was estimated to be less than 0.025 mm (0.001 in.) in 40 hr of engine operations.

Direct flow measurements were not available. The pressure drops at each comparable compressor discharge pressure setting were higher for the brush seal system than for the labyrinth seal system, implying that for the same engine operating conditions the dual-brush system leaked less than the baseline forward-facing labyrinth seal system. Also implied is enhanced engine efficiency.

More efficient seals cannot simply be installed into an engine without computing and accounting for the secondary airflows necessary for the cooling and engine dynamics associated with the seal leakage modifications.

## ACKNOWLEDGMENTS

The authors wish to thank Chris Conrad, Edward Chisolm, Dan Erbacher, Dave Evanoff, Joe Flowers, Stephen Grozner, Tim Hawk, Teresa Kline, Paul Lemermeier, Karl Owen, Edith Parrott, Jeffry Paulin, Barry Piendl, Joe Shivak, Don Striebing, Queito Thomas, and the Corpus Christi T–700 Engine Assembly Area.

## REFERENCES

Childs, D.W., Ramsey, C.J., and Pelletti, J.M., 1989, "Rotordynamic-Coefficient Test Results for the SSME HPOTP Turbine Interstage Seal for the Current and Improved Swirl Brake," NASA Lewis Grant NAG3–181, Turbomachine Laboratories Report 338–TL–3–89, Texas A&M University, College Station, TX 77843.

Demko, J.A., Morrison, G.L., and Rhode, D.L., 1988, "The Prediction and Measurement of Incompressible Flow in a Labyrinth Seal," AIAA Paper No. 88–0190.

Flower R., 1990, "Brush Seal Development Systems," AIAA Paper 90–2143.

Hendricks, R.C., Carlile, J.A., and Liang, A.D., 1992, "Some Sealing Concepts—A Review. Part A–Industrial, Proposed, and Dynamic; Part B–Brush Seal Systems," Presented at the ISROMAC–4, The Fourth International Symposium of Transport Phenomena and Dynamics of Rotating Machinery, Honolulu, Hawaii, U.S.A., Apr. 5–8.

Morrison, G.L., and Chi, D., 1985, "Incompressible Flow in Stepped Labyrinth Seals," ASME Paper No. 85–FE–4.

Rhode, D.L., Ko, S.H., and Morrison, G.L., 1988, "Numerical and Experimental Evaluation of a New Low Leakage Labyrinth Seal," AIAA/ASME/SAE/ASEE 24th Joint Propulsion Conference, July 11–13, 1988, Boston, MA, Paper No. 88–2884.

Stocker, H.L., Cox, D.M., and Holle, G.F., 1977, "Aerodynamic Performance of Conventional and Advanced Design Labyrinth Seals With Solid-Smooth, Abradable, and Honeycomb Lands," NASA CR–135307.

Trutnovsky, K., 1977, "Contactless Seals. Foundations and Applications of Flows Through Slots and Labyrinths," NASA TT F 17352.

## TABLE I.—T–700 COMPRESSOR DISCHARGE SEAL AND ENGINE TEST PARAMETERS

(a) On way up

| Configuration | Compressor speed, rpm | Turbine speed, rpm | Compressor discharge pressure, psia | Compressor discharge low-pressure-cavity exhaust (CDLPCE) temperature, °F | Impeller aft cavity pressure, psia | CDLPCE pressure, psia | Pressure difference, psia |
|---|---|---|---|---|---|---|---|
| Baseline | 29 600 | 10 500 | 50 | 348 | 37.5 | 16.2 | 21.3 |
| Brush | | | | 321 | 39.5 | 15.4 | 24.1 |
| Difference | | | | | | | 2.8 |
| Baseline | 35 500 | 14 000 | 70 | 498 | 46.7 | 17.0 | 29.7 |
| Brush[a] | | | 79 | 458 | 53.1 | 16.3 | 36.8 |
| Difference | | | | | | | 7.1 |
| Baseline | 38 300 | 17 400 | 90 | 578 | 57.5 | 18.4 | 39.1 |
| Brush | | | | 502 | 59.2 | 16.8 | 42.4 |
| Difference | | | | | | | 3.3 |
| Baseline | 41 300 | 20 000 | 120 | 688 | 74.2 | 21.2 | 53.0 |
| Brush | 40 400 | 20 000 | | 599 | 76.0 | 18.7 | 57.3 |
| Difference | | | | | | | 4.3 |
| Baseline | 43 190 | 19 000 | 145 | 765 | 87.6 | 23.9 | 63.7 |
| Brush | 42 340 | 20 000 | | 673 | 89.9 | 20.8 | 69.1 |
| Difference | | | | | | | 5.4 |
| Baseline and brush | 43 090 | 19 700 | 155 | 710 | 95.6 | 21.8 | 73.8 |

(b) On way down

| | | | | | | | |
|---|---|---|---|---|---|---|---|
| Baseline and brush | 42 500 | 20 000 | 145 | 683 | 89.9 | 20.9 | 69.0 |
| Baseline | 41 400 | 20 000 | 120 | 690 | 74.1 | 21.2 | 52.9 |
| Brush | | | | 605 | 76.4 | 18.9 | 57.5 |
| Difference | | | | | | | 4.6 |
| Baseline | 38 400 | 17 400 | 90 | 581 | 57.7 | 18.5 | 39.2 |
| Brush | 37 800 | 18 100 | | 516 | 59.1 | 16.9 | 42.2 |
| Difference | | | | | | | 3.0 |
| Baseline | 35 600 | 14 000 | 70 | — | 46.8 | 16.9 | 29.9 |
| Brush | 34 800 | 14 600 | | 473 | 48.2 | 16.0 | 32.2 |
| Difference | | | | | | | 2.3 |
| Baseline | 29 700 | 10 500 | 50 | 378 | 37.6 | 16.1 | 21.5 |
| Brush | 31 700 | 10 500 | 59 | 379 | 42.9 | 15.8 | 27.1 |
| Difference | | | | | | | 5.6 |

[a]rpm overshot and then backed down to "run through" the compressor critical speed. (Note: this is not the case on the way down.)

## TABLE II.—RELATIVE PRESSURE DROPS FOR BASELINE COMPRESSOR DISCHARGE LABYRINTH AND BRUSH SEAL SYSTEMS

(a) On way up

| Compressor discharge pressure, psia | Pressure difference, $\Delta P_{brush} - \Delta P_{baseline}$, psi |
|---|---|
| 50 | 2.8 |
| [a]70, [b]79 | 7.1 |
| 90 | 3.3 |
| 120 | 4.3 |
| 145 | 5.4 |

(b) On way down

| | |
|---|---|
| 120 | 4.6 |
| 90 | 3.0 |
| 70 | 2.3 |
| [a]50, [b]59 | 5.6 |

[a]Baseline.
[b]Brush.

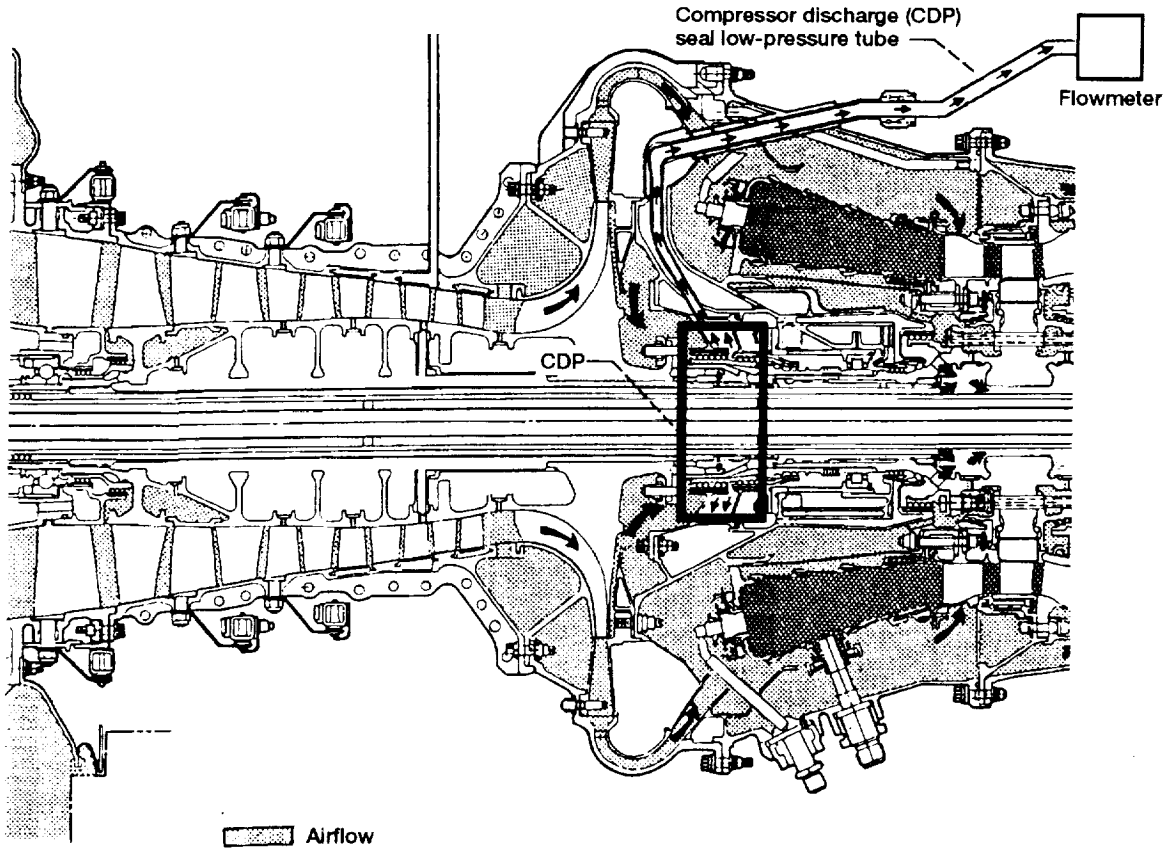


(a) Airflow schematic.

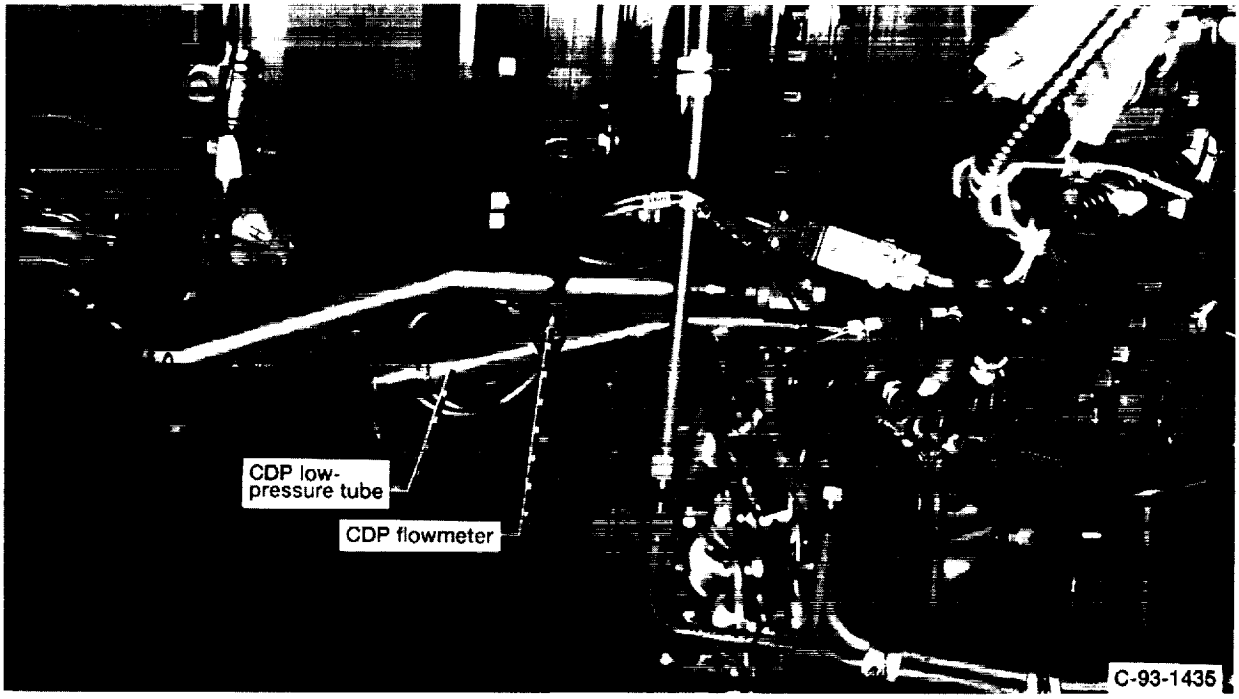


(b) Location of CDP flowmeter.

Figure 1.—Schematic of engine airflow and location of flowmeter.

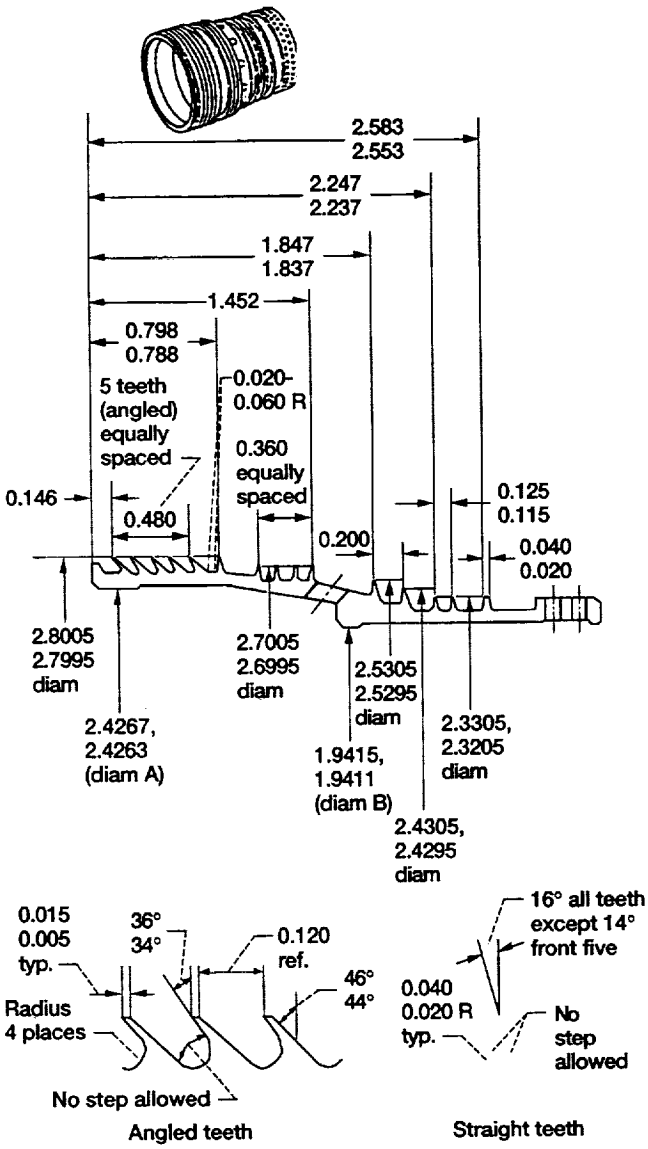


Figure 2.—Schematic of labyrinth compressor discharge seal system. (Seal teeth and axis established by diameters A and B to be concentric within 0.003 full indicator reading. No steps allowed on tooth face or at fillet radius. All dimensions are in inches.)


Figure 3.—Simulated exploded view of labyrinth compressor discharge seal system.

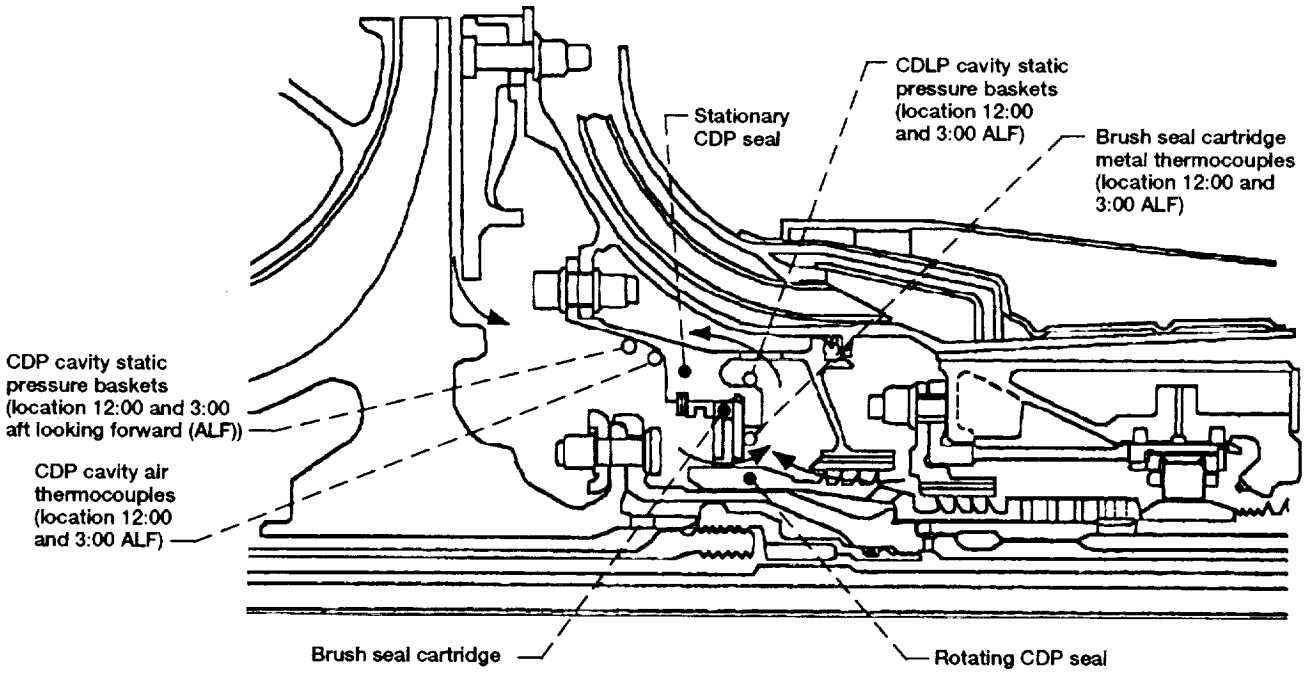


(a) Brush seal package and airflow.

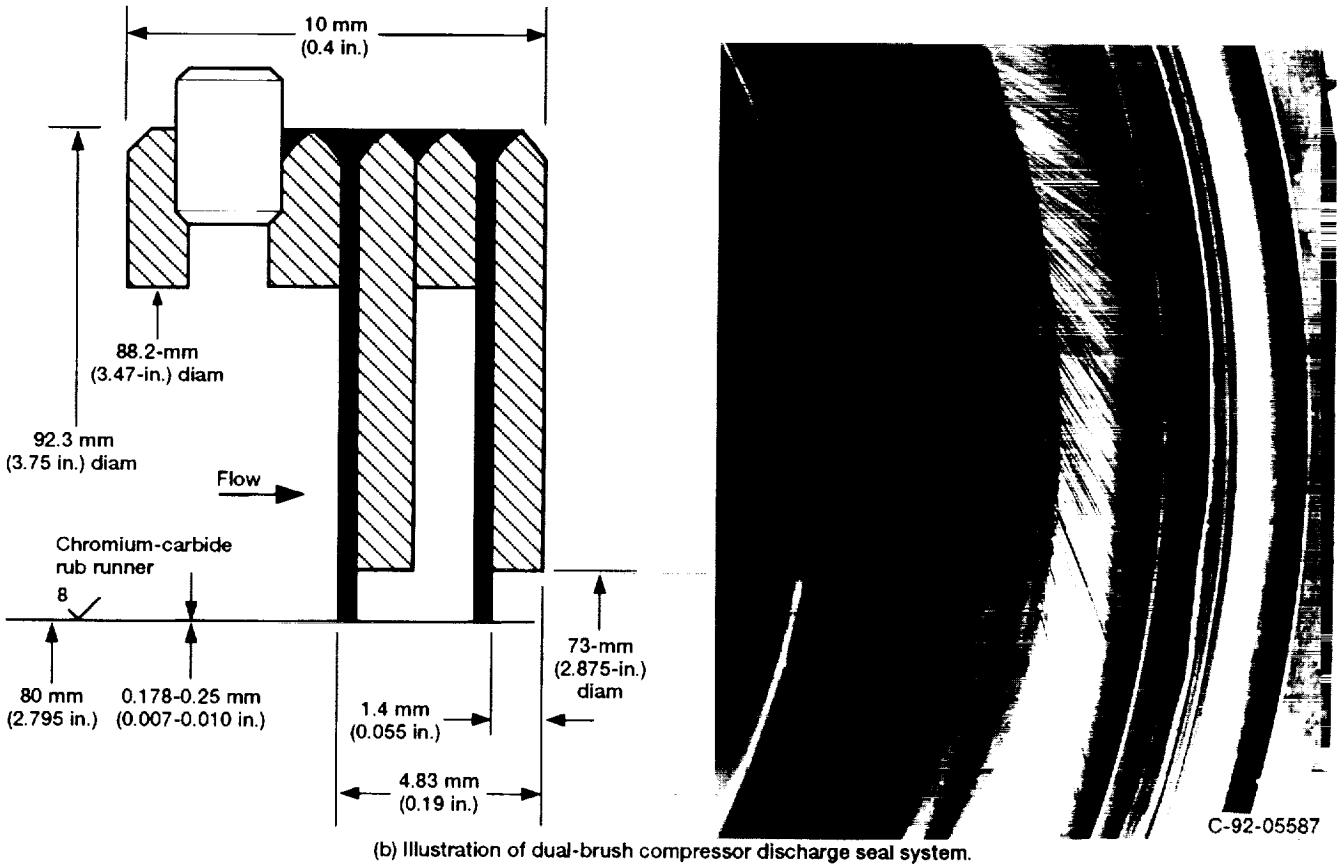


(b) Illustration of dual-brush compressor discharge seal system.

Figure 4.—Dual-brush compressor discharge seal system and schematic of airflow.

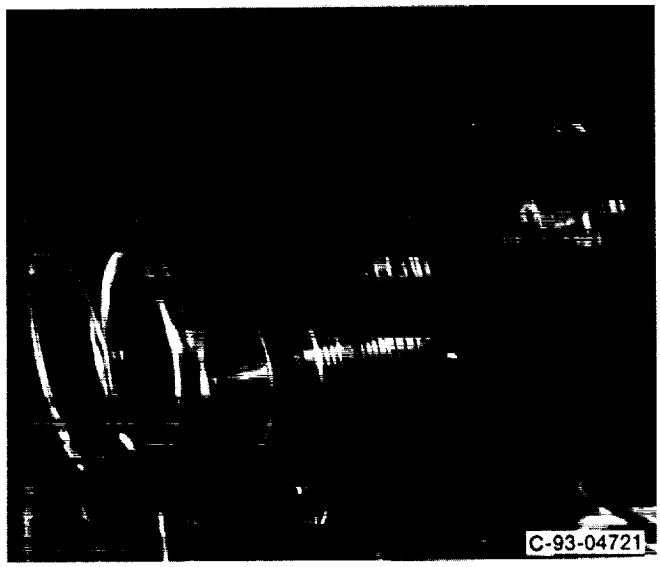


Figure 5.—Exploded view of dual-brush compressor discharge seal system (after test).

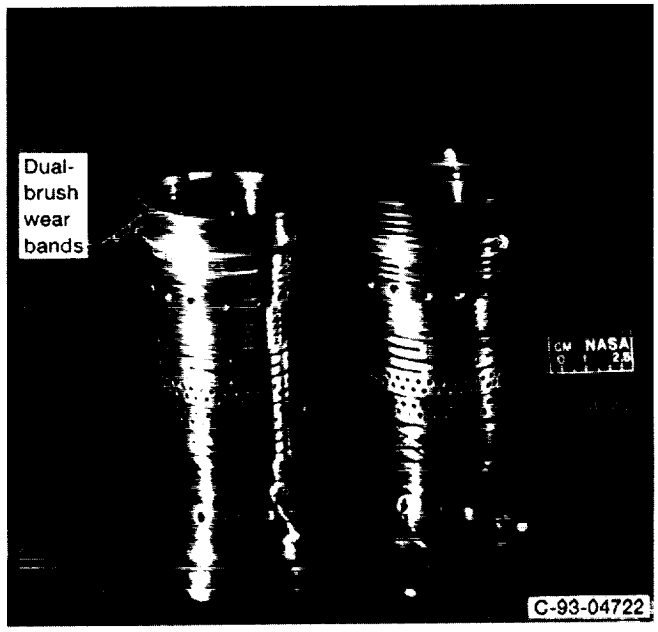


Figure 6.—Compressor discharge seal rotors for labyrinth seal (right) and brush seal (left).

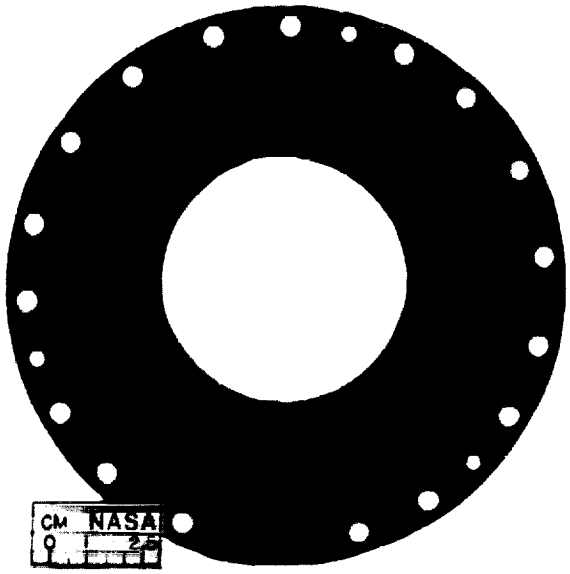


C-93-02710

(a) Upstream view.

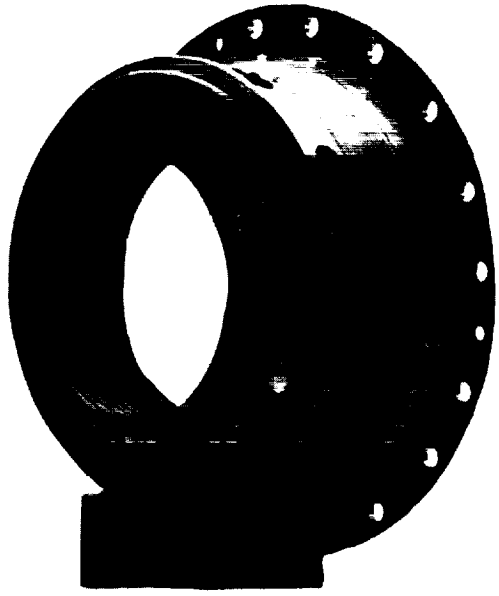

C-93-02712

(b) Downstream view.

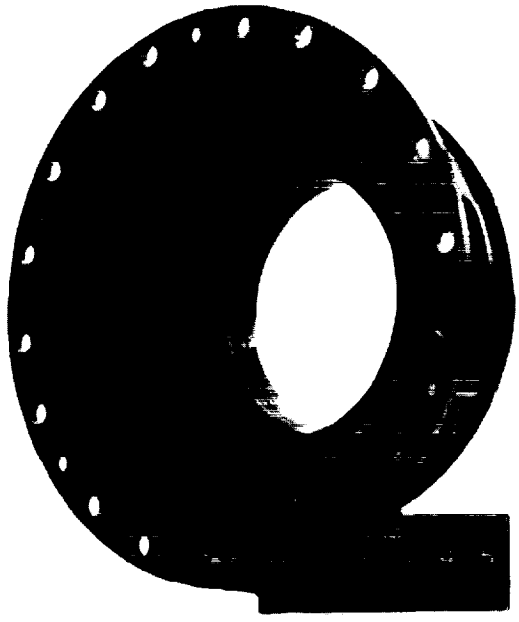

C-93-02711

(c) Isometric view.

Figure 7.—Dual-brush compressor discharge seal system after testing.

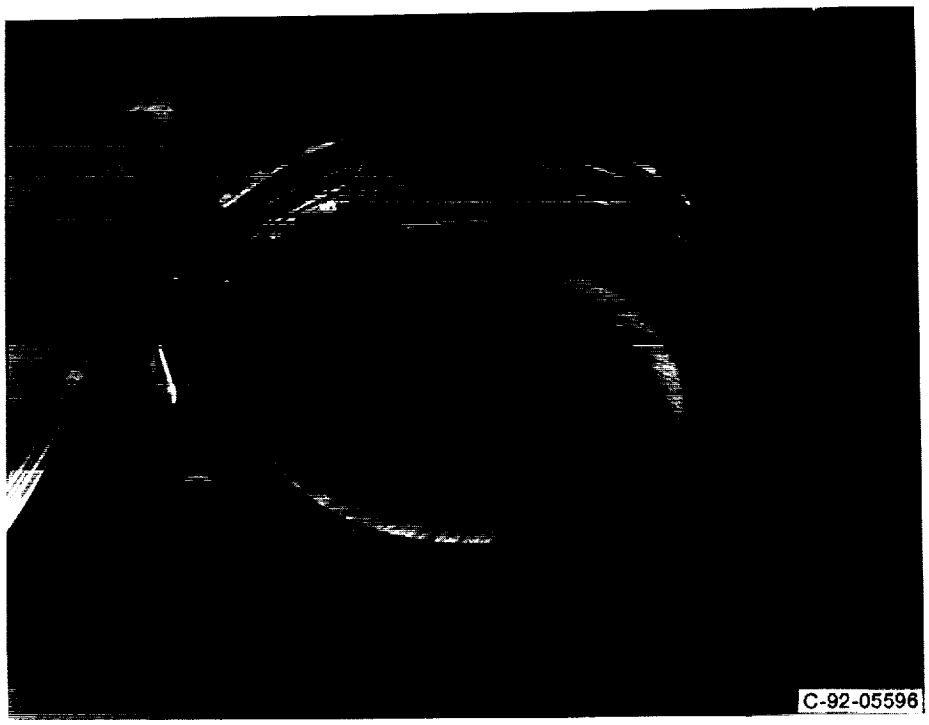


(a) Dual-brush seal.

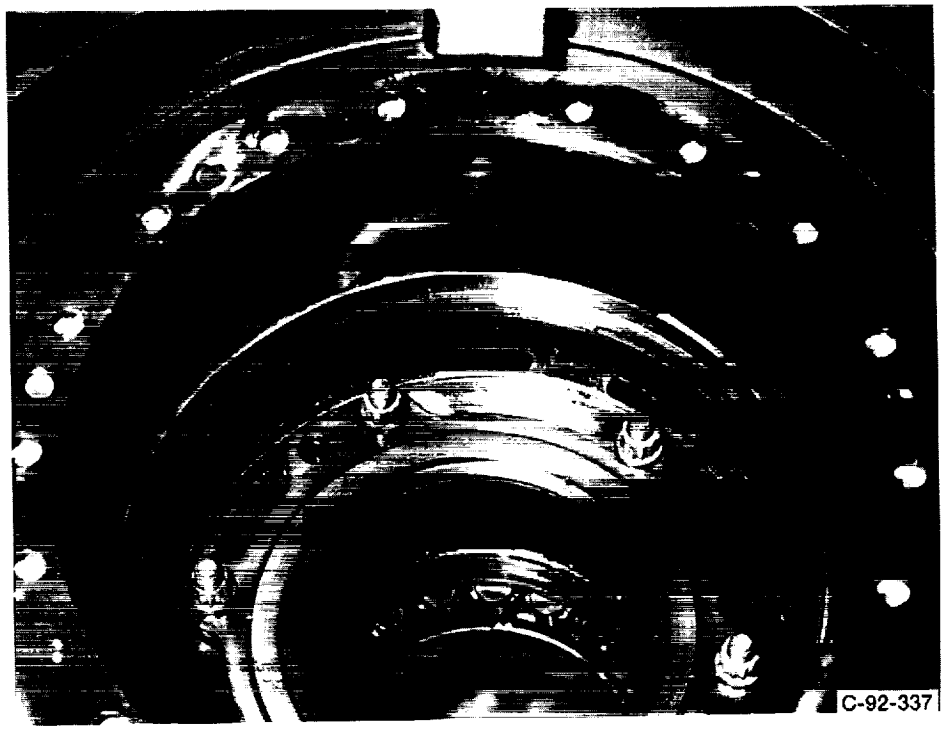


(b) Seal package cavity and housing.

Figure 8.—Dual-brush seal package installation.

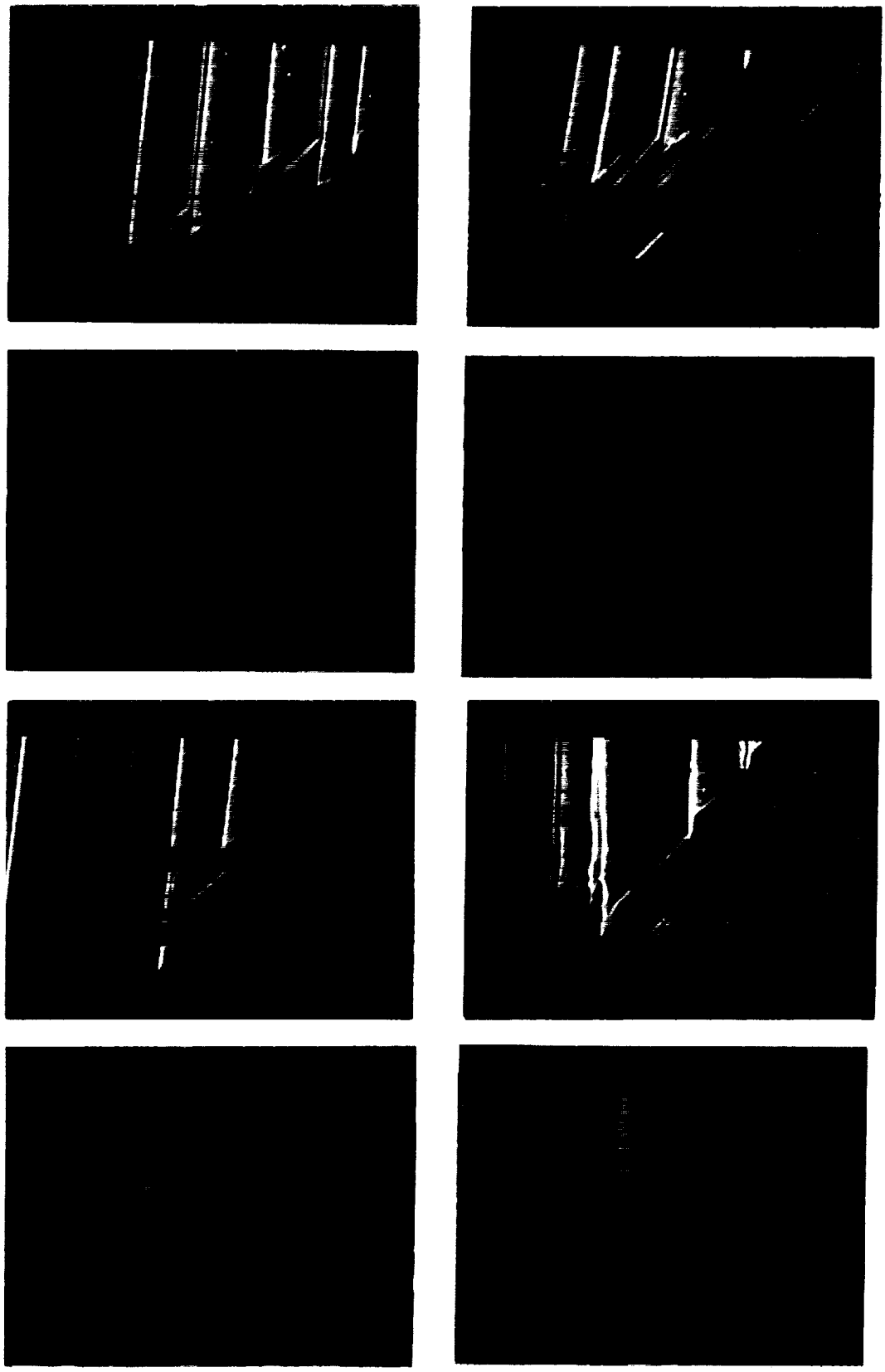

Figure 9.—Closeup views of bristles.

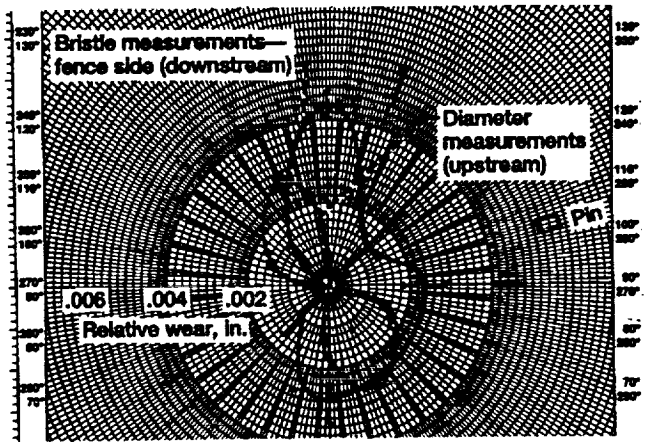


Figure 10.—Wear pattern for compressor discharge seal upstream brush.

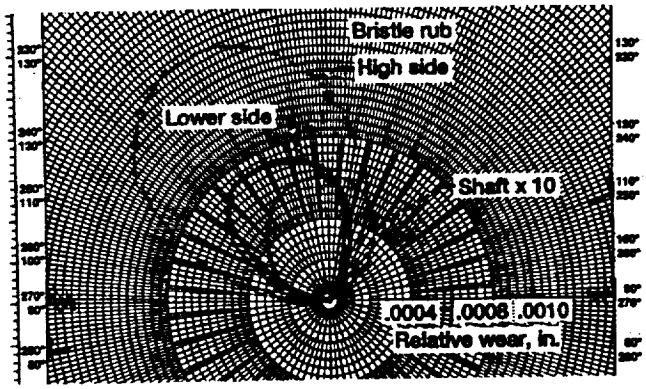


Figure 11.—Coating wear pattern for compressor discharge seal rub runner.

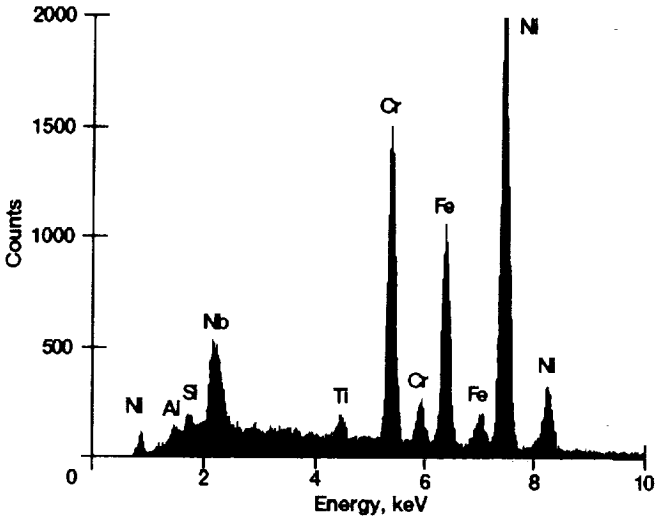


(a) Particle A.

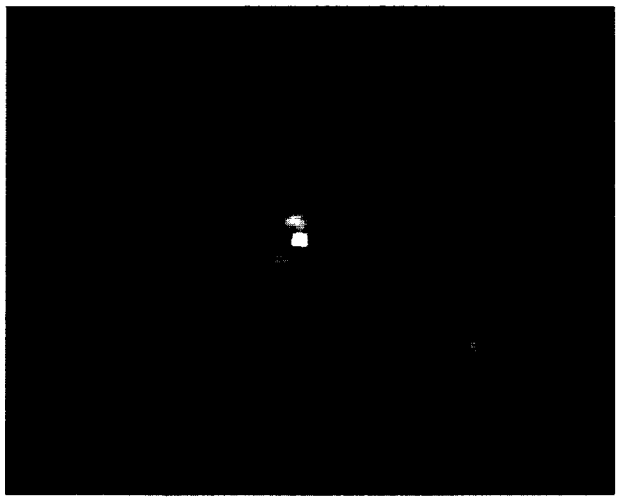

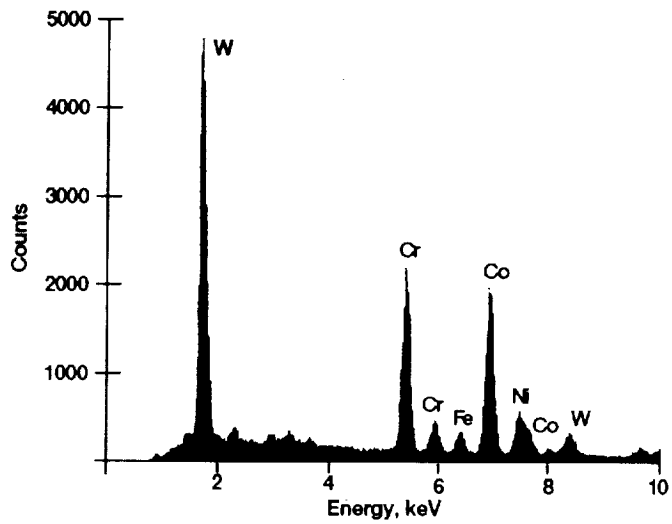


(b) Particle B.

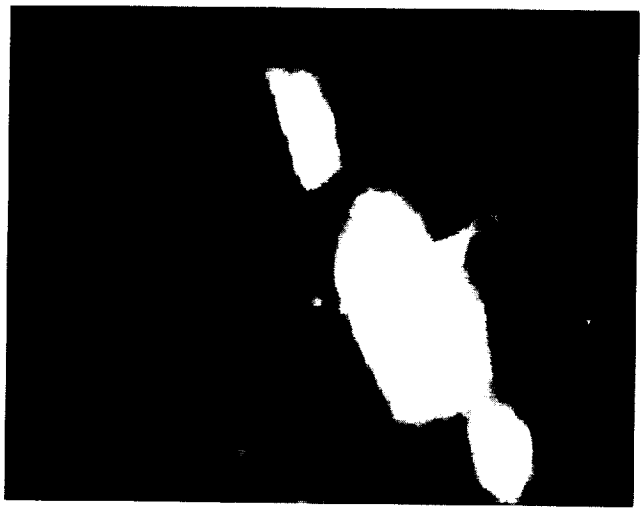

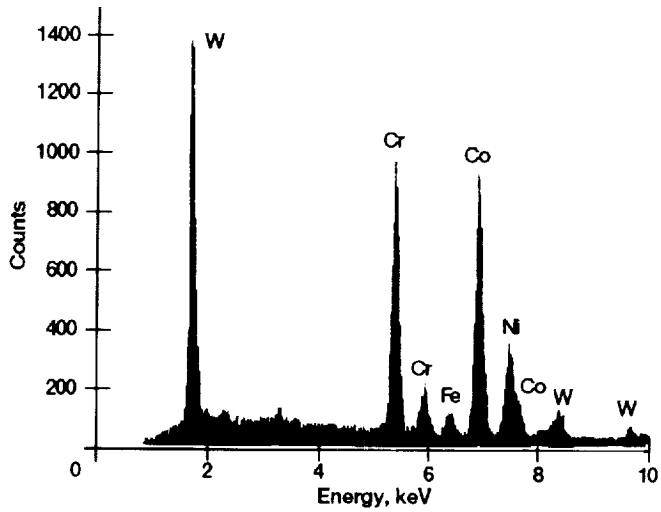


(c) Particle C.

Figure 12.—SEM peaks associated with drain pipe debris.

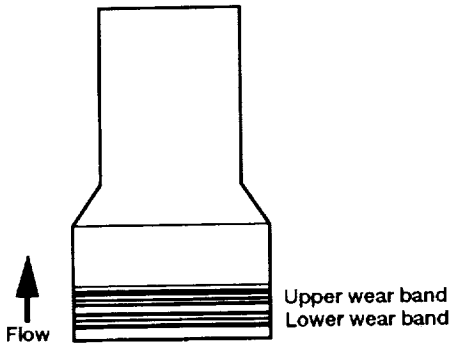


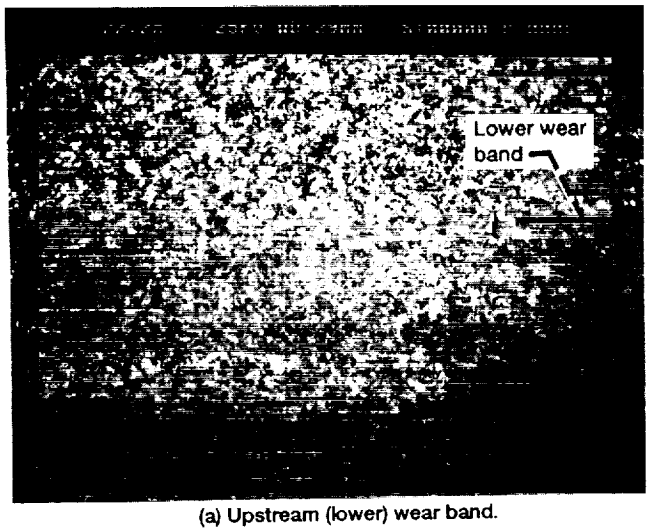


(a) Upstream (lower) wear band.

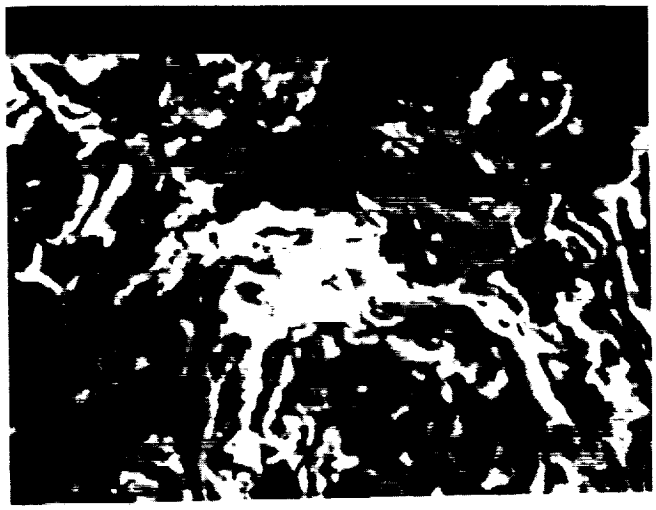

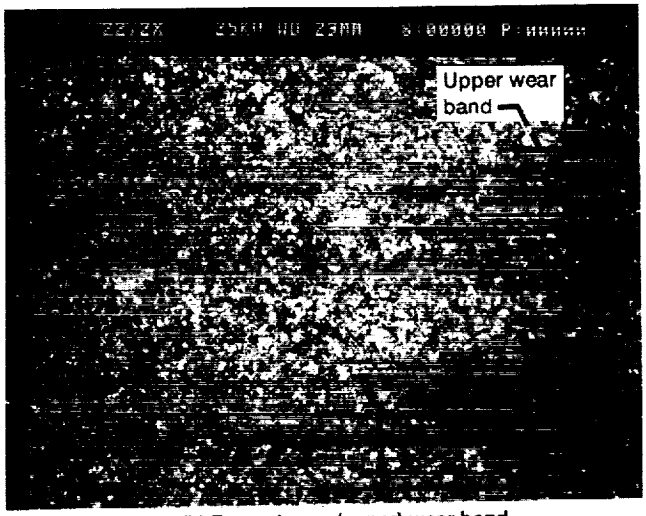


(b) Downstream (upper) wear band.

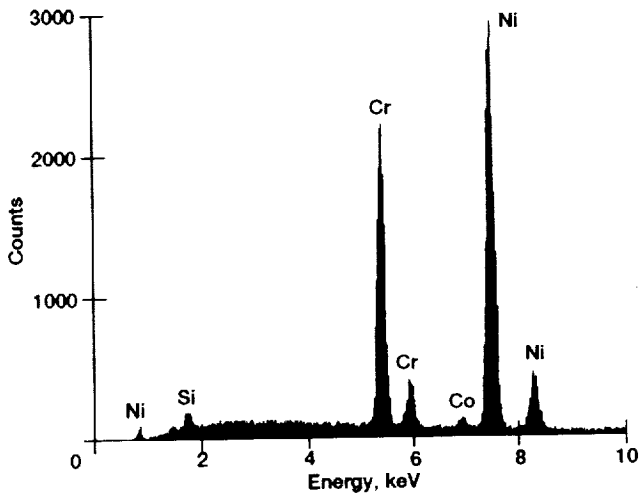


(c) Light area in coating matrix between bands.

Figure 13.—SEM peaks associated with chromium-carbide-coated rub runner.

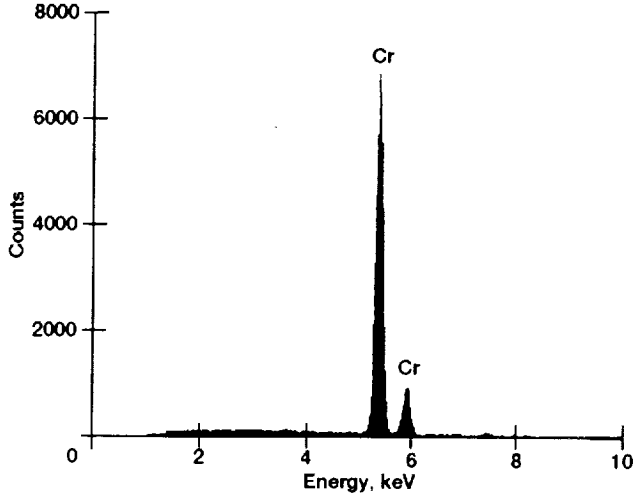


(d) Gray area in coating matrix between bands.

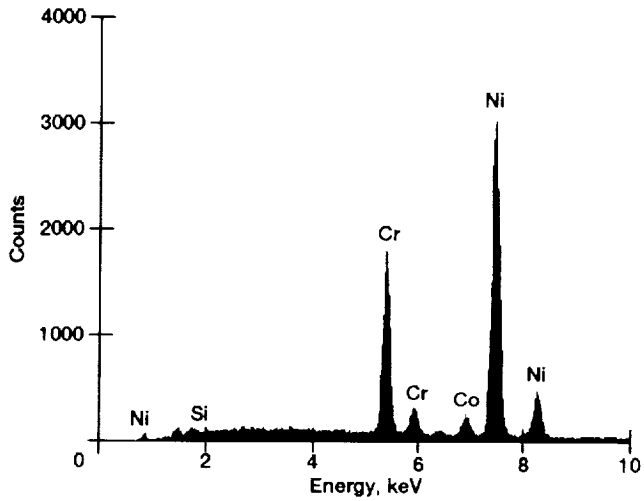


(e) Light area in upstream (lower) wear band.

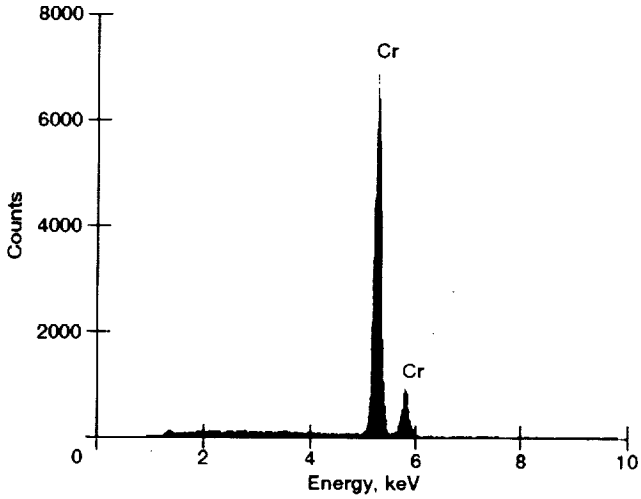


(f) Gray area in upstream (lower) wear band.

Figure 13.—Continued.

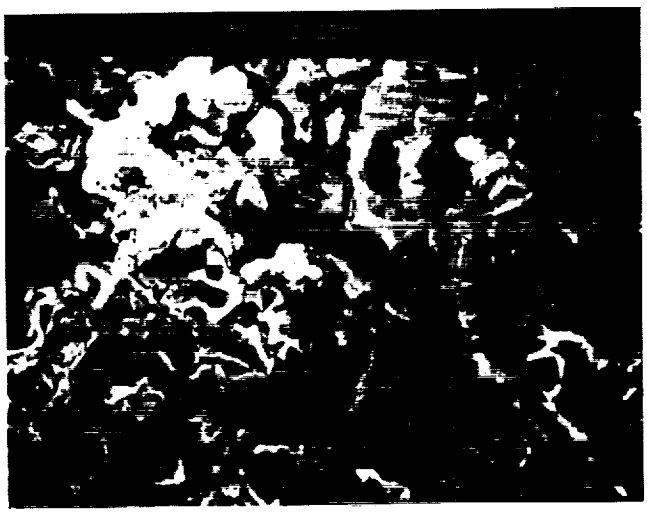

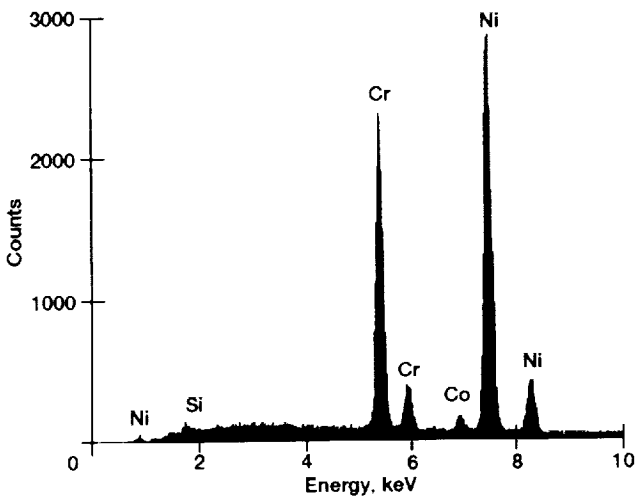


(g) Light area in downstream (upper) wear band.

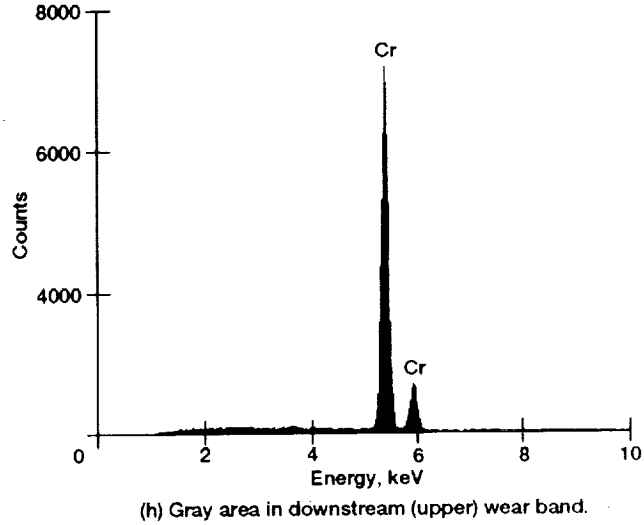


(h) Gray area in downstream (upper) wear band.

Figure 13.—Concluded.